ELSEVIER

Biochimica et Biophysica Acta 1271 (1995) 304–314

BBA Biochimica et Biophysica Acta

The amino-terminal peptide of HIV-1 glycoprotein 41 fuses human erythrocytes

Patrick W. Mobley [a], Hsing-Fang Lee [a], Cyril C. Curtain [b], Alan Kirkpatrick [c], Alan J. Waring [d], Larry M. Gordon [d,*]

[a] *Chemistry Department, California State Polytechnic University, Pomona, Pomona, CA, USA*
[b] *Department of Physics, Monash University, Clayton, Victoria, Australia*
[c] *CSIRO Division of Biomolecular Engineering, Parkville, Victoria, Australia*
[d] *Department of Pediatrics, King-Drew Medical Center / UCLA, Los Angeles, CA, USA*

Received 6 July 1994; revised 13 January 1995; accepted 27 January 1995

Abstract

The ability of synthetic peptides based on the amino-terminus of HIV-1 glycoprotein 41 000 (gp41) to fuse human erythrocytes was investigated. Previous site-directed mutagenesis studies have shown an important role for the N-terminal gp41 domain in HIV-fusion, in which replacement of hydrophobic amino acids with polar residues inhibits viral infection and syncytia formation. Here, a synthetic peptide (FP; 23 amino acid residues 519–541) corresponding to the N-terminus of HIV-1 gp41, and also a FP analog (FP526L/R) with Arg replacing Leu-526, were prepared with solid phase techniques. The lipid mixing and leakage of resealed ghosts triggered by these peptides were examined with fluorescence quenching techniques. Peptide-induced aggregation of human erythrocytes was studied using Coulter counter sizing and scanning electron microscopy (SEM). Using resealed erythrocyte ghosts at physiologic pH, FP induces rapid lipid mixing between red cell membranes at doses previously shown to hemolyze intact cells. FP also causes leakage from resealed ghosts, and promotes the formation of multicelled aggregates with whole erythrocytes. Contrarily, similar FP526L/R concentrations did not induce red cell lysis, lipid mixing, leakage or aggregation. Since the fusogenic potency of FP and FP526L/R parallels earlier gp41 mutagenesis studies showing that substitution of Arg for Leu-526 blocks fusion activity, these data suggest that the N-terminal gp41 domain in intact HIV participates in fusion.

Keywords: Fusion; Lysis; Erythrocyte; HIV; AIDS; HIV glycoprotein 41 000 (gp41); Membrane; Red cell; Peptide; Melittin; Ca^{2+}

1. Introduction

Recent evidence supports the hypotheses that the amino-terminal peptide (approx. 23 amino acid residues 519–541 [1]) of glycoprotein 41 000 (gp41) plays critical roles in the fusion and cytopathic processes underlying HIV-1 infection of target cells [2]. With myxoviruses and paramyxoviruses, the fusion site on the viral envelope protein is a conserved hydrophobic amino acid sequence at the amino terminus of the F_1 protein [3]. Gallaher [4] and Gonzalez-Scarano et al. [5] each noted extensive homologies of these sequences with those of the N-terminus of gp41, and suggested that the N-terminal gp41 peptide is similarly involved in the fusion of the HIV envelope with host cells. According to a recent model [6,7], the viral envelope gp41 might act as a 'bridge,' fusing the target cell surface bilayer through the N-terminal sequence of gp41 with the HIV lipid bilayer [8,9]. Indeed, Koenig et al. [10] suggested that HIV infection of cells occurs only if the amino-terminal peptide interacts with the target cell membrane, perhaps by destabilizing the lipid bilayer. Experimental support for these hypotheses comes from site-

Abbreviations: PBS, phosphate-buffered saline; DMSO, dimethyl sulfoxide; HIV-1, Human Immunodeficiency Virus, Type-1; gp41, glycoprotein 41 000 of HIV-1; gp120, glycoprotein 120 000 of HIV-1; FP, HIV amino-terminal peptide 519–541 of gp41; FP526L/R, a FP analog in which Leu-526 is replaced by Arg; HIV-L, C-terminal peptide 828–855 of gp41; SEM, scanning electron microscopy; R_{18}, octadecyl rhodamine B chloride; ANTS, aminonapthalene-1,3,6-trisulfonic acid; DPX, *p*-xylene-bis-pyridinium bromide; VSV, vesicular stomatitis virus; RBC, red blood cells; SUV, small unilamellar vesicles; LUV, large unilamellar vesicles; POPG, 1-palmitoyl-2-oleoyl phosphatidylglycerol; POPC, 1-palmitoyl-2-oleoyl phosphatidylcholine; DOPC, dioleoylphosphatidylcholine; DOPE, dioleoylphosphatidylethanolamine; K_D, dissociation constant.

* Corresponding author. Fax: +1 (310) 668 3407.

SSDI 0925-4439(95)00048-8

directed mutagenesis studies showing that substitution of hydrophobic amino acids with polar residues in the N-terminal peptide lowered the infectivity of HIV and its ability to promote syncytium formation [11–14]. The N-terminal gp41 peptide might also directly kill target cells [4], thereby contributing to the decline of $CD4^+$ lymphocytes that is a clinical hallmark of AIDS. Consistent with this view is the finding that a mutation affecting the amino-terminal sequence of HIV-1 gp41 produced a much less cytopathic virus [15].

Although the use of site-specific mutated HIV-1 is a powerful tool for investigating the functional role(s) of viral envelope epitopes, further studies with complementary techniques are needed before unequivocally assigning fusogenic and cytolytic activities to the N-terminal domain of gp41. In particular, Larsen et al. [16] noted that control experiments were not done in the above studies to show that site-specific mutations do not significantly perturb the overall gp41 structure. Furthermore, site-specific mutations of either the V3 region of gp120 [14] or gp41 regions outside the N-terminal domain [14,17,18] inhibit postbinding fusion activities; this suggests that envelope protein regions other than the N-terminus of gp41 also contribute to the fusion process in the intact virus.

An alternative experimental approach that focusses exclusively on the membrane actions of the N-terminal domain of HIV-1 gp41 involves the use of synthetically-prepared peptides. For example, addition of synthetic peptides (i.e., 23-residue sequence 519–541 [19,20] or 16-residue sequence 519–534 [21]) to model liposomes induced lipid-mixing. Possibly related to this fusogenic activity is the finding with light scattering that the 23-residue sequence 519–541 mediated liposome aggregation [19,20]. Further, the 23-residue peptide 519–541 [19,20] and 16-residue peptide 519–534 [22] from HIV-1 gp41 each induced leakage of lipid vesicles. Of particular interest is the finding that the 23-residue peptide 519–541 induced mixing of aqueous lipid vesicle contents [20]. However, before these findings with liposomes can be legitimately extrapolated to HIV infection processes, further studies examining the biomembrane actions of the N-terminal gp41 peptide are required using human cells.

In the present paper, the respective abilities of the synthetic N-terminal peptide of HIV-1 gp41 (FP; 23 residues 519–541) and a site-substituted FP (FP526L/R; Arg replacing Leu-526) to fuse and lyse human red cell membranes are investigated. Previously, we have shown that FP lysed both intact human erythrocytes and $CD4^+$-lymphocytes [23]. In further physical-biochemical experiments on human red cells, we reported that the N-terminal HIV-1 gp41 peptide may achieve these lytic effects by forming peptide aggregates in the red cell membrane [6]. The control peptide FP526L/R was chosen because a prior mutagenic study indicated that replacement of Leu-526 with Arg completely blocked syncytium formation, using $CD4^+$ HeLa cells transfected with HIV *env* glycoprotein expression vectors [12]. Synthetic FP, but not FP526L/R, agglutinated red cells, and also triggered lipid-mixing and leakage of resealed erythrocyte ghosts. These data indicate that addition of synthetic peptides to red cells may provide a model system for understanding FP-membrane interactions underlying HIV fusion processes.

2. Materials and methods

2.1. Materials

Bee-venom melittin was from Sigma Chemical (St. Louis, MO) and was used without further purification. Octadecyl rhodamine B chloride (R_{18}), aminonapthalene-1,3,6-trisulfonic acid (ANTS) and the quencher *p*-xylene-bis-pyridinium bromide (DPX) were from Molecular Probes (Eugene, OR). Triton X-100, $CaCl_2$, MOPS, L-histidine, DMSO, EDTA, NaCl and bovine serum albumin were from Sigma Chemical (St. Louis, MO).

The 23-amino acid N-terminal sequence of gp41 (FP; NH_2-Ala-Val-Gly-Ile-Gly-Ala-Leu-Phe-Leu-Gly-Phe-Leu-Gly-Ala-Ala-Gly-Ser-Thr-Met-Gly-Ala-Arg-Ser-$CONH_2$) of the HIV-1 strain LAV_{1a}, and also a site-substituted FP analog (FP526L/R; NH_2-Ala-Val-Gly-Ile-Gly-Ala-Leu-Phe-**Arg**-Gly-Phe-Leu-Gly-Ala-Ala-Gly-Ser-Thr-Met-Gly-Ala-Arg-Ser-$CONH_2$), were synthesized and purified as described earlier [23]. FP encompasses amino acid residues 519–541 of HIV-1 gp41 [1]. The expected molecular masses of FP and FP526L/R were obtained by fast-atom bombardment mass spectrometry and electrospray mass spectrometry (UCLA Center for Molecular and Medical Sciences Mass Spectrometry). Quantitative amino acid compositions for the peptides were determined at the UCLA Protein Microsequencing Facility.

2.2. Preparation of human red blood cells (RBC)

Human red blood cells (RBC) were prepared using outdated units from the local blood bank [23]. All units tested negative for antibodies to HIV-1, and hepatitis B and D. Red cells were washed three times in 0.85% NaCl, and packed cells from the last wash were suspended in isotonic (phosphate-buffered saline (PBS)) buffer, consisting of 120 mM NaCl-2.7 mM KCl-10 mM Na_2HPO_4 (pH 7.4).

2.3. Hemolysis assays of human red blood cells

For testing of peptide-induced hemolysis, small aliquots (≤ 10 μl) of concentrated FP, FP526L/R or melittin in 100% DMSO were added to 0.5 ml of the isotonic PBS buffer to yield the desired peptide concentration. For Ca^{2+}-induced hemolysis, small aliquots (≤ 25 μl) of a concentrated calcium stock buffer (i.e., 200 mM $CaCl_2$ in

isotonic PBS) were added to 0.5 ml of isotonic PBS buffer and cells to yield the desired Ca^{2+} concentration. Aliquots (10 μl) of the packed, washed cells were then added, and after 30 min at 37° C, the suspension was centrifuged at approx. 5000 × g for 1.5 min and the supernatant analyzed spectrophotometrically for hemoglobin at 543 nm [7,24]. Percent lysis was calculated, using a reference of the average of three tubes in which 10 μl of packed cells were incubated in 0.5 ml of distilled water for the duration of the experiment. Control experiments indicate that the highest concentration of carrier DMSO (i.e., 2.6%) did not increase hemolysis.

2.4. Preparation of resealed human red blood cell ghosts

Lysed and resealed red cell ghosts were prepared according to the method of Sze and Solomon [25], with several modifications. Packed human red blood cells were washed three times in the PBS buffer with centrifugation at 2500 × g for 10 min (5000 rpm with a JA-20 rotor in a Beckman Model J2-21 centrifuge). The cells were then allowed to hemolyze for 30 min in 8 vol. of 5 mM sodium-phosphate, pH 7.4. The ghosts were pelleted by centrifugation at 22000 × g for 20 min (approx. 15000 rpm with the JA-20 rotor). The supernatant was removed with a tap aspirator. The pellet was washed three more times with the 5 mM sodium-phosphate, pH 7.4 buffer, and suspended in a minimum volume (approx. 0.5 ml) of this buffer. The creamy white-pink ghosts were stored at 4° C. Protein assays were performed using the Bio-Rad protein assay reagent (Richmond, CA) and bovine serum albumin as standard.

Sealed ghosts were prepared by resuspending the lysed cells in 4–5 vol. of resealing buffer (120 mM KCl/30 mM NaCl/10 mM sodium phosphate, pH 7.4) containing 0.75 mM sucrose. The mixture was incubated on ice for 15 min, and the ghosts were subsequently resealed at 37° C in the presence of 1 mM Mg^{2+} for 45 min. Nonentrapped sucrose was removed by repeated centrifugation at 15000 rpm for 20 min each time. The final pellet, sucrose-loaded resealed ghosts, was suspended in the appropriate incubation buffer.

For leakage experiments, the above protocol for preparing resealed ghosts was modified to include fluorescent dye and fluorescence quencher during the resealing step (see below).

2.5. Lipid-mixing (fusion) assay

Lipid-mixing between red cell membranes was quantitated from the relief of fluorescence self-quenching of the membrane-incorporated fluorescent probe, octadecyl rhodamine B chloride (R_{18}). Fusion of R_{18}-labeled red blood cell ghosts with unlabeled ghosts reduces the membrane surface-density of the fluorophore, thereby producing an increase in fluorescence intensity [26].

For lipid-mixing experiments, the resealed ghosts were divided into two equal portions: one aliquot was stored on ice, while the other had R_{18} added and was then incubated for 1 h at a final concentration of 1 mol R_{18}/50 mol of red cell lipid under vortexing at room temperature. The labeled, resealed ghosts was incubated in the dark for one hour at room temperature. Unincorporated R_{18} was removed by gel filtration on a Sephadex G-75 column (incubation buffer: 120 mM KCl/30 mM NaCl/10 mM Na_2HPO_4/0.1 mM EDTA), and the unlabeled, resealed ghosts were diluted to the same volume as the labeled, resealed ghosts collected from the column.

Fluorescence intensities were recorded using a Perkin-Elmer 650-40 fluorescence spectrophotometer at 37° C. For fusion measurements, zero fluorescence (F_0) was taken as the emission intensity at 590 nm (560 nm, excitation wavelength) of the labeled and unlabeled resealed ghosts (1:1) before the fusion agent is added, and 100% fluorescence (F_{100}) is the corresponding intensity after the incubation medium is made 1% Triton X-100. F_s represents the fluorescence intensity, measured for a 1:1 mixture of labeled and unlabeled, resealed ghosts on addition of the putative fusion agent for the indicated time. Accordingly, the percent fusion may be defined as

$$\%Fusion = 100 \times [(F_s - F_0)/(F_{100} - F_0)] \quad (1)$$

2.6. Leakage from resealed ghosts

Leakage was measured with a fluorescence assay of resealed red blood cell ghosts containing both the water-soluble fluorescent marker ANTS and the quencher DPX. Upon membrane leakage with addition of a putative lytic agent, ANTS and DPX are released to the buffer medium. This effectively dilutes the quencher concentration, thereby increasing the fluorescence intensity of ANTS [27].

For leakage experiments, ANTS and DPX were incorporated into the ghosts during the resealing step (see above). The resealed ghosts initially contain both ANTS (12.5 mM) and DPX (45 mM). Non-encapsulated ANTS/DPX was removed by centrifugation at 22000 × g (approx. 15000 rpm), 8° C for 20 min. The pellet was suspended in 1 ml of running buffer (100 mM NaCl/2 mM MOPS/2 mM L-histidine/1 mM EDTA; pH 7.4), for each 1 ml of lysed ghosts. This ghost solution (30 μl) was mixed with the leakage agents and running buffer to a total volume of 1.5 ml. Fluorescence intensity of this 1.5 ml mixture was measured at 37° C at 767 nm, with an excitation wavelength at 384 nm. The initial fluorescence intensity for ghosts resealed with ANTS (12.5 nm) and DPX (45 mM) is zero; an increase in the fluorescence intensity recorded for these resealed ghosts is proportional to the degree of membrane leakage. Leakage results are presented as Delta (Emission Intensity) at 767 nm, which is equal to the intensity recorded with a putative lytic agent subtracted by the corresponding intensity recorded with only the carrier solvent.

2.7. Coulter counter sizing of human erythrocytes

The aggregation state of human red blood cells was assessed with Coulter counter sizing. Aliquots (10 μl) of washed, packed red blood cells were incubated in 0.5 ml PBS with the indicated agent at 37° C for 30 min. Agents were added as described above for hemolysis assays. At the end of the incubation an aliquot of the mixture was diluted 1:50000 in isotonic PBS in a 20 ml disposable blood vial (Baxter Diagnostics, Irwine, CA). Particle numbers in each of 16 size ranges were determined with a Coulter Counter-Model ZBI (Coulter Electronics, Hileah, FL), equipped with a stirrer. The total particle volume (V_T) was calculated as the summation, over each of the 16 channels, of the number (N_C) of particles in each channel multiplied by the maximum particle volume (V_{MC}) in each channel. % Total volume in each channel is then defined as:

$$\%Total\ Volume = 100 \times [(N_C \times V_{MC})]/V_T] \quad (2)$$

2.8. Scanning Electron Microscopy (SEM) of human erythrocytes

Samples were prepared for Scanning Electron Microscopy (SEM) by the method of Birch et al. [28]. Red cells were taken from the hemolysis assay and fixed in 2.5% glutaraldehyde for 1 h at room temperature. The fixed cells were placed on poly-L-lysine coated cover slips. After a 1 hr treatment with 2% osmium tetroxide, the sample was washed and dehydrated by 5 stepwise increases (at least 15 min each) in aqueous ethylene glycol from 20 to 95%. Two further changes of 60% and 95% cellosolve in ethylene glycol and three of absolute cellosolve prepared the sample for critical point drying. Critical point drying was conducted in a 1250J critical point dryer from Pelco (Redding, CA). The Scanning Electron Microscope was an Amray 1000A (Bedford, MA).

3. Results

3.1. FP- and FP526L/R-induced fusion (lipid-mixing) of resealed human erythrocyte ghosts

Fluorescence measurements were carried out to assess the lipid-mixing effects of the amino-terminal peptide of gp41 (FP) on resealed erythrocyte ghosts. These assays rely on the fact that the fluorochrome R_{18} is heavily self-quenched when inserted in a membrane lipid bilayer at high fluorochrome/lipid (approx. 1:100). In the absence of lipid mixing, the dye only very slowly transfers from the bilayers of the labeled resealed ghosts to those of the unlabeled resealed ghosts. When lipid-mixing fusion occurs, the dye is rapidly diluted throughout the system and relief of self-quenching results in an increase in fluorescence. In initial time-course studies at 37° C, R_{18}-labeled and -unlabeled resealed ghosts were incubated with 30 μM FP for various times (Fig. 1). Earlier experiments showed that 30 μM FP-induced approx. 40% lysis of human red blood cells [23]. Maximum lipid-mixing occurred in approx. 7 min with 30 μM FP, and this plateau was maintained for at least another 18 min (Fig. 1). Control experiments in Fig. 1 indicated that the highest concentration of carrier solvent (2.6% DMSO) did not promote lipid mixing; the 'zero' time lipid mixing was identical with or without 2.6% DMSO.

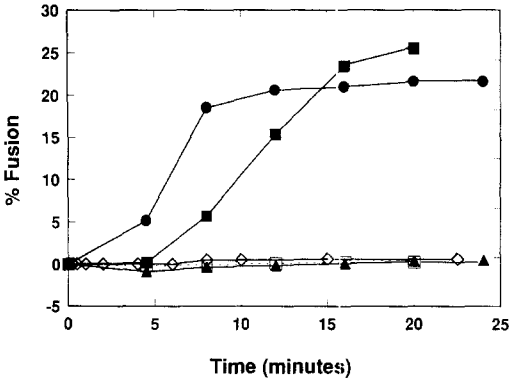

Fig. 1. Time dependence of lipid mixing induced by the amino terminal peptide of HIV-1 gp41 (FP), a FP analog (FP526L/R) in which Arg is substituted for Leu-526, melittin or calcium using resealed human erythrocyte ghosts at 37° C. Percent fusion is measured by the increase in fluorescence of the lipid-soluble probe, octadecyl rhodamine B chloride (R_{18}), due to relief of self-quenching upon fusion of labeled and unlabeled resealed ghosts (see Section 2). Complete (100%) fusion is taken as the maximal fluorescence resulting from treatment with 1% Triton X-100. R_{18}-labeled (200 μl) resealed ghosts and unlabeled (200 μl) resealed ghosts were incubated with the agent for the indicated times at 37° C in the incubation buffer (pH 7.4; 120 mM KCl/30 mM NaCl/10 mM Na_2HPO_4/0.1 mM EDTA). The total volume was 1.5 ml. The agents tested were: FP (30 μM; ●-●), FP526L/R (34 μM; ◇-◇), melittin (5 μM; ▲-▲), Ca^{2+} (2 mM; ■-■) and DMSO (2.6%; □-□). FP, FP526L/R and melittin were each added to the incubation mixture from a DMSO (100%) stock solution, yielding the above peptide concentration and 2.6% DMSO. Excitation and emission wavelengths were 560 and 590 nm, respectively. Results are means of duplicate determinations, and are representative of three independent experiments.

For comparative purposes, the site-substituted analog of FP (FP526L/R) and two hemolytic agents (melittin and 2 mM $CaCl_2$) were tested for their effects on lipid mixing between resealed erythrocyte ghosts. Fig. 1 shows that FP526L/R, at a concentration (34 μM) slightly higher that used for FP, does not induce lipid-mixing; in parallel hemolysis experiments (data not shown), we found that 34 μM FP526L/R produced less than 5% lysis of intact erythrocytes when incubated for 30 min. Melittin, at a 5 μM peptide dosage that achieves 100% hemolysis [23], also did not promote lipid-mixing between resealed ghosts for the duration (24 min) of the experiment (Fig. 1). On the other hand, addition of 2 mM $CaCl_2$ induced lipid-mixing similar to that of 30 μM FP, with maximal lipid-mixing occurring at approximately 15 min. The ability of 2

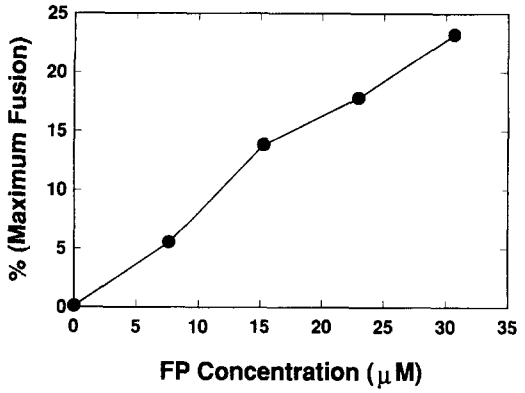

Fig. 2. Dose-dependent effects of the amino terminal peptide of HIV-1 gp41 (FP) on the lipid-mixing of resealed human erythrocyte ghosts at 37° C. The 'zero' point reflects the lipid-mixing noted with the carrier concentration of DMSO (2.6%). R_{18}-labeled (200 μl) resealed ghosts and unlabeled (200 μl) resealed ghosts were incubated with the agent for 20 min at 37° C in the isotonic buffer of Fig. 1. % Fusion is defined from Eqn. 1. Results are means of duplicate determinations, and are representative of three independent experiments.

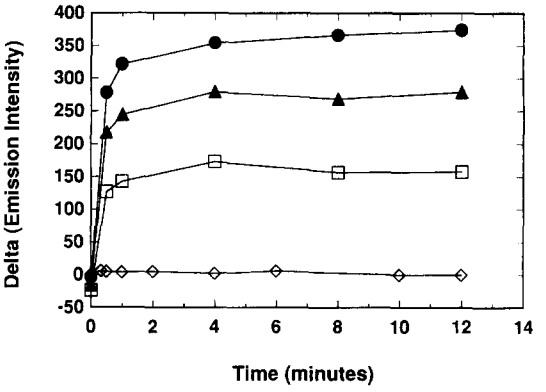

Fig. 3. Time dependence of leakage from resealed human erythrocyte ghosts induced by the amino terminal peptide of HIV-1 gp41 (FP) and the FP analog (FP526L/R) at 37° C. The Delta (Emission Intensity) is equal to the fluorescence intensity at 767 nm recorded with a putative lytic agent subtracted by the corresponding intensity recorded with only the carrier solvent (≤ 2.6% DMSO). Delta (Emission Intensity) is proportional to the release of ANTS and DPX from the resealed ghosts. Resealed ghosts (30 μl) containing 12.5 mM ANTS and 45 mM DPX were incubated with either FP526L/R (34 μM; ◇) or the following μM concentrations of FP: 15 (□); 30 (▲); and 45 (●). Results are means of duplicate determinations, and are representative of three independent experiments.

mM $CaCl_2$ to induce lipid-mixing noted in Fig. 1 is consistent with previous fusion studies by Hoekstra et al. [29], which indicated this $CaCl_2$ concentration also promotes contents mixing of resealed ghosts. In separate experiments, we found that incubation of 2 mM $CaCl_2$ with intact red cells produced approx. 25% hemolysis (data not shown).

Since FP-induced lipid-mixing is maximal at 20 min in Fig. 1, this incubation time was used in the dose-response lipid-mixing curve for the peptide. Fig. 2 shows that FP induces a dose-dependent lipid-mixing of human red blood cells, with 24% lipid-mixing occurring at 30 μM. It is of interest that a similar dose-response curve was obtained previously for FP-induced hemolysis of human red blood cells [23].

3.2. FP- and FP526L/R-induced leakage from resealed human erythrocyte ghosts

The ability of FP and FP526L/R to cause leakage of internal contents of resealed ghosts was examined with a fluorescent assay developed by Ellens et al. [27]. Here, ghosts were resealed with the fluorochrome ANTS and the quencher DPX, and leakage of ANTS and DPX into the medium is monitored by the fluorescence increase of unquenched ANTS. Fig. 3 shows that 15 μM FP induces rapid leakage of the resealed ghosts, attaining the plateau within approx. 1 min after peptide addition. Comparable time-courses for leakage were noted for resealed ghosts incubated with 30 and 45 μM FP, with the following order for the maximal release of ANTS and DPX: 15 μM FP < 30 μM FP < 45 μM FP (Fig. 3). Contrarily, experiments with 34 μM FP526L/R indicated no leakage when the site-substituted FP analog was added to resealed ghosts (Fig. 3). Although the FP concentrations that induce leakage of resealed ghosts are similar to those for lipid-mixing (Figs. 1 and 2) and hemolysis [7,23], it should be noted that maximal leakage of resealed ghosts occurs much faster than either maximal lipid-mixing of resealed ghosts (approx. 7 min; Fig. 1) or maximal hemolysis of intact red cells (approx. 30 min; see Mobley et al. [23]).

It is of interest to contrast FP-induced leakage of resealed ghosts with that caused by either melittin or $CaCl_2$. The time-courses for peptide-induced leakage in Fig. 4 indicate that either 1 μM or 2 μM melittin does not

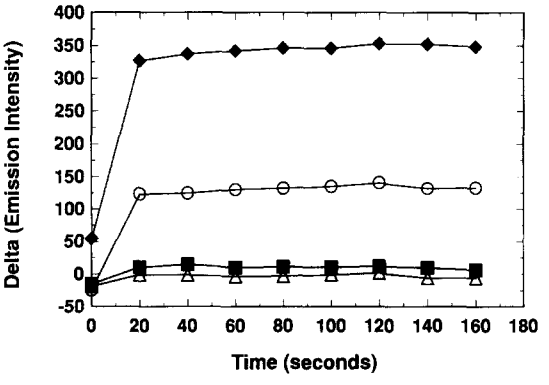

Fig. 4. Time dependence of leakage from resealed human erythrocyte ghosts induced by bee-venom melittin at 37° C. The Delta (Emission Intensity) is equal to the fluorescence intensity at 767 nm recorded with a putative lytic agent subtracted by the corresponding intensity recorded with only the carrier solvent (≤ 2.6% DMSO). Delta (Emission Intensity) is proportional to the release of ANTS and DPX from the resealed ghosts. Resealed ghosts (30 μl) containing 12.5 mM ANTS and 45 mM DPX were incubated with the following μM concentrations of melittin: 1 (△); 2 (■); 5 (○); and 10 (◆). Results are means of duplicate determinations, and are representative of three independent experiments.

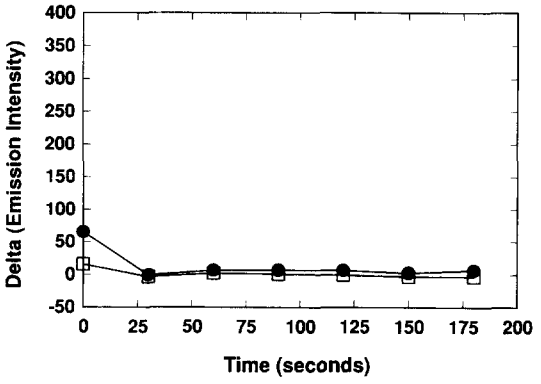

Fig. 5. Time dependence of leakage from resealed human erythrocyte ghosts induced by $CaCl_2$ at 37° C. The Delta (Emission Intensity) is equal to the fluorescence intensity at 767 nm recorded with a putative lytic agent subtracted by the corresponding intensity recorded with only the running buffer (see Section 2). Delta (Emission Intensity) is proportional to the release of ANTS and DPX from the resealed ghosts. Resealed ghosts (30 μl) containing 12.5 mM ANTS and 45 mM DPX were incubated with the following mM concentrations of $CaCl_2$: 5 (□); and 10 (●). Results are means of duplicate determinations, and are representative of three independent experiments.

trigger significant release of contents from resealed ghosts. However, 5 μM and 10 μM melittin each produce rapid leakage of resealed ghosts, reaching their respective plateaus in 20 s (Fig. 4). Accordingly, the maximal leakage induced by FP (Fig. 3) or that triggered by 5 or 10 μM melittin (Fig. 4) proceed rapidly, each being completed within 1 min. It should also be noted that the maximal leakage of resealed ghosts induced by 5 or 10 μM melittin occurs much faster than maximal hemolysis of red cells (i.e., approx. 30 min; see Mobley et al. [23]). Further, resealed ghosts appear to be much more resistant to melittin-induced lysis than whole red cells: 2 μM melittin lyses 100% of red blood cells, but has no impact on leakage of resealed ghosts (Fig. 4; Mobley et al. [23]). These findings suggest that the mechanisms underlying FP- (or melittin-) induced hemolysis and leakage from resealed ghosts are different. A further indication that hemolysis and leakage of resealed ghosts reflect distinct phenomena are the findings that $CaCl_2$, at 5 mM and 10 mM doses that hemolyze red blood cells, had no effect on the leakage of contents from resealed ghosts (Fig. 5).

3.3. FP- and FP526L/R-induced aggregation of human red blood cells

Since the above results showed that N-terminal HIV-1 gp41 peptide mediates both fusogenic and cytolytic activity with resealed erythrocyte ghosts, FP and FP526L/R were also tested for aggregation of human red cells. Coulter counter experiments were conducted on washed, packed red blood cells incubated in the isotonic PBS buffer with FP, FP526L/R, melittin and Ca^{2+} for 30 min (Fig. 6). Counts were made for particles in channels ranging in maximum particle volume (μ^3) from 2 to 4,224. A plot of the % (Total Volume) versus the maximum particle volume is shown in Fig. 6, where % (Total Volume) is the percent fraction of the red cell particle volume in a given channel to the total volume of the particles in all channels (see Section 2). For 30 μM FP and DMSO (2.6%), this plot is nearly symmetrical with the largest % (Total Volume) value occurring with a maximum particle volume of 528 μ^3. Control experiments with either PBS or DMSO (2.6%) indicated much smaller particle sizes for red blood cells. Specifically, the 66 μ^3 channel has the largest % (Total Volume) for red cells treated with either PBS or DMSO. The simplest interpretation of these data is that FP

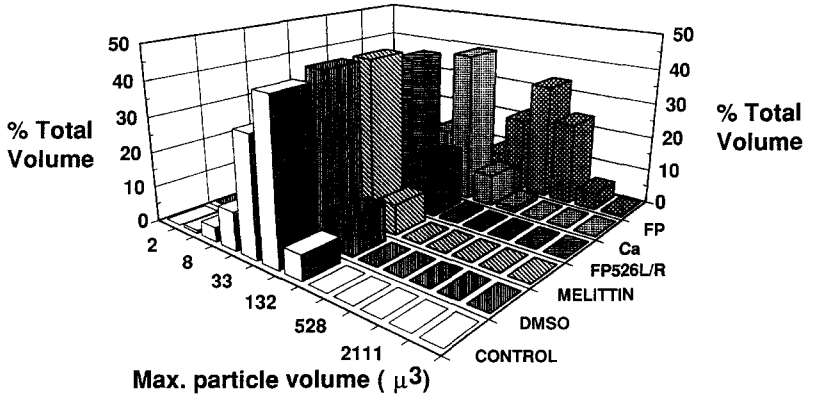

Fig. 6. Coulter counter sizing of erythrocytes treated with the amino terminal peptide of HIV-1 gp41 (FP), the FP analog (FP526L/R), Ca^{2+}, or melittin. Erythrocytes were tested for aggregation by incubating 10 μl of packed red blood cells, diluted to 0.5 ml in PBS buffer, with the following agents at 37° C for 30 min: 34 μM FP and DMSO (2.6%) (cross-hatch bars); 2 mM $CaCl_2$ (dotted bars); 44 μM FP526L/R (narrow diagonal bars) and DMSO (2.6%); 1.5 μM melittin and DMSO (2.6%) (broad diagonal bars); and 2.6% DMSO (vertical bars). The control was run by adding 10 μl of PBS buffer (white bars). At the end of the incubation, an aliquot of the mixture was diluted 1:50000 in isotonic phosphate-buffered saline. The number of particles in each of the 12 size ranges (i.e., maximum particle volume μ^3, x axis) shown was then determined with a Coulter counter. No particles were found in the four channels with the largest maximum particle volumes (e.g., 8448, 16900, 33798 and 67000 μ^3), and were omitted from this plot. Percent (Total Volume) for the particles in each channel (z axis) is calculated as in Section 2. Results are means of duplicate determinations, and are representative of three independent experiments.

induces variable aggregations of erythrocytes. If it is assumed, as a first approximation, that the volume of an individual red cell is not substantially altered by FP incubation, then the mean number of single red cells in the aggregates of the 528 μ^3 channel is equal to 8 (i.e., = 528 μ^3 (FP-treated)/66 μ^3 (DMSO or PBS control)). Consistent with the interpretation that FP triggers aggregation of red cells is the finding that FP-treatment decreases the number (N) of particles by approx. 5-fold (i.e., 333 334 (PBS control) to 65 839 (FP-incubated), where N is sampled from the standard assay with 10 μl of packed red cells). The other fusogenic agent, 2 mM $CaCl_2$, induces a more modest volume increase in the erythrocyte particles; here, the channel with the largest % (Total Volume) increases from 66 to 132 μ^3 (Fig. 6). Contrarily, neither melittin (1.5 μM) nor FP526L/R (44 μM) and DMSO (2.6%) altered the particle sizes of human erythrocytes (Fig. 6), in agreement with these peptides not being fusogenic (Fig. 1).

Scanning electron microscopy (SEM) studies on FP-treated human erythrocytes confirmed that this peptide facilitated aggregation of red cells (Fig. 7). Control experiments on red cells treated with DMSO (2.6%) showed separate cells that principally share the normal discoid shape characteristic of erythrocytes, with occasional echinocyte projections (Fig. 7A,C). Incubation with the amino-terminal HIV-1 gp41 peptide exerts profound effects on red cell morphology. Fig. 7B shows only multicell aggregates, in agreement with the above Coulter counter sizing results. At higher magnification, Fig. 7D indicates that the individual cells in the aggregates are distorted and elongated. Although these morphological perturbations may be a consequence of both hemolysis and membrane fusion, the absence of severely disrupted membranes in Fig. 7B,D

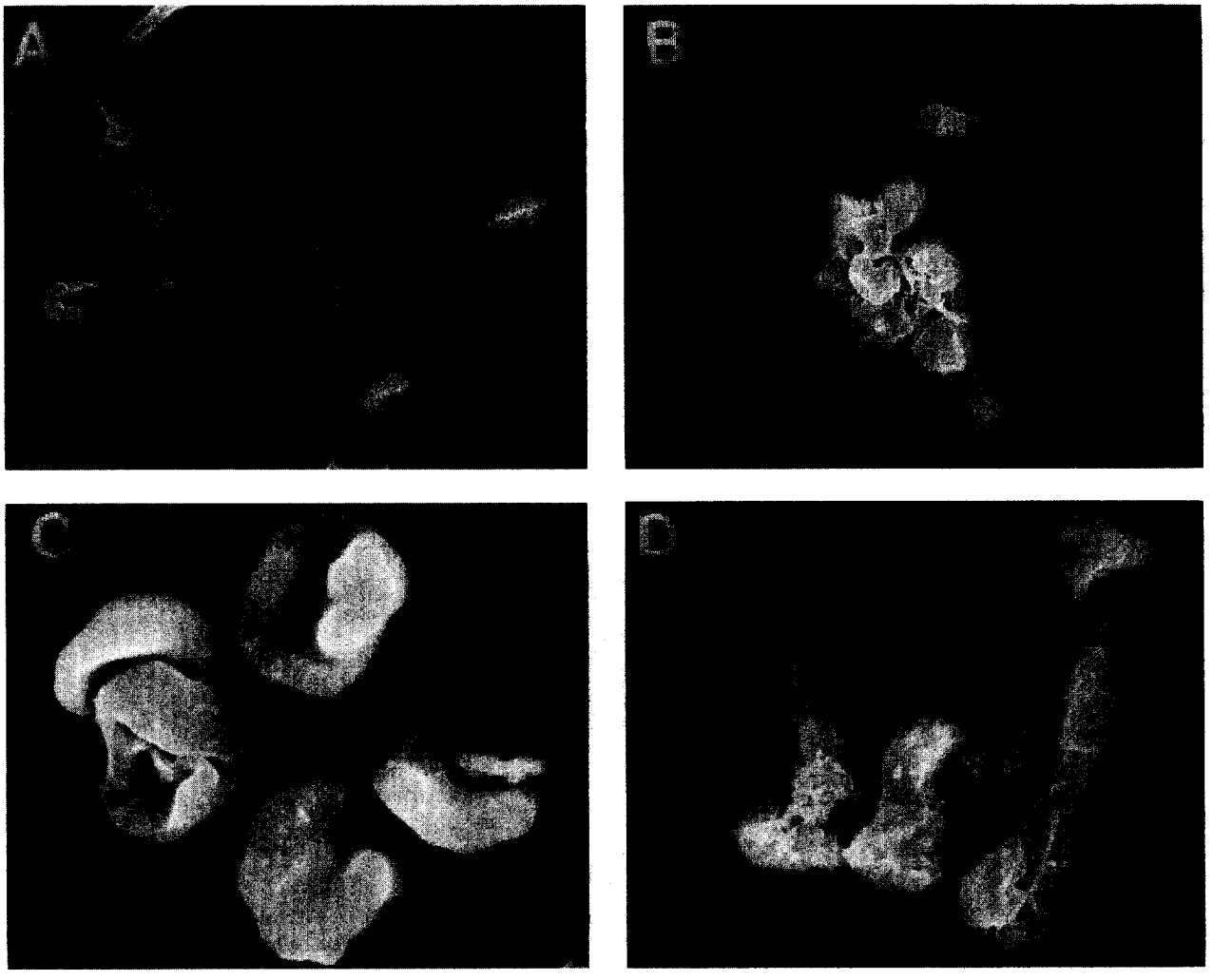

Fig. 7. Scanning Electron Microscopy (SEM) of human red blood cells treated with the amino-terminal peptide of HIV-1 gp41 (FP). (A) Control red cells suspended in isotonic PBS and incubated for 30 min with DMSO (2.6%). The white bar at the top is equal to 2 μm; (B) Red cells suspended in isotonic PBS and incubated for 30 min with 34 μM FP and DMSO (2.6%). The white bar at the top is equal to 2 μm; (C) Control red cells suspended in isotonic PBS and incubated for 30 min with DMSO (2.6%). The white bar at the top is equal to 0.8 μm; (D) Red cells suspended in isotonic PBS and incubated for 30 min with 34 μM FP and DMSO (2.6%). The white bar at the top is equal to 1.14 μm. Fields chosen are representative of three independent experiments.

argues against FP producing these effects through chaotropic, 'detergent-like' actions.

4. Discussion

In this study, we show for the first time that the synthetic amino-terminal peptide of HIV-1 gp41 (FP) promotes fusion of a biological membrane. Specifically, FP triggered lipid mixing of resealed erythrocyte ghosts, and also caused multicellular aggregates. These results should be compared with previous model liposome studies using fusion peptides derived from the amino-terminal peptide of HIV gp41 [19–21]. In early work with the synthetic HIV-1 fusion peptide Rafalski et al. [19] noted that the 23-residue gp41 sequence 519–541 (FP) catalyzed lipid mixing in small unilamellar vesicles (SUV) containing negatively-charged phospholipids (POPG), but not neutral phospholipids (POPC). More recently, FP was reported to induce lipid-mixing between the large unilamellar vesicles (LUV) of negatively-charged POPG, but only if Ca^{2+} or Mg^{2+} were first added to the lipid [20]; Nieva et al. [20] suggested that the lipid-mixing activity of FP with SUV of POPG noted by Rafalski et al. [19] may be due to the inherent strain in the packing of bilayer lipids in such small vesicles. In the absence of divalent cations, Martin et al. [21] observed that the 16-residue gp41 peptide 519–534 induced lipid intermixing of LUV containing phosphatidylethanolamine. Similarly, FP induced fusion of LUV containing DOPC/DOPE/cholesterol (1:1:1) in a buffer lacking divalent cations [20]. Our results showing that FP caused lipid-mixing between resealed erythrocyte ghosts in the absence of divalent cations corresponds most closely with the above LUV-containing phosphatidylethanolamine findings [20,21], since red cell membranes also have a low membrane curvature and contain substantial amounts of phosphatidyl ethanolamine [8].

Here, we also report that FP induces aggregation for human red cells suspended in buffers lacking divalent cations, as indicated by Coulter counter sizing studies and Scanning Electron Microscopy (SEM) (Figs. 6 and 7). Previously, Rafalski et al. [19] showed that FP caused aggregation of acidic (POPG) and neutral (POPC) SUV liposomes in the absence of divalent cations. On the other hand, FP did not aggregate negatively-charged POPG LUV, unless Ca^{2+} or Mg^{2+} was first added to the buffer [20]. However, Nieva et al. [20] observed that FP could induce aggregation of LUV containing DOPC/DOPE/cholesterol (1:1:1) in a buffer without divalent cations, consistent with our results that FP aggregated red cells.

The leakage of resealed ghosts induced by FP supports previous studies indicating that this viral peptide is lytic. The dose-response curve noted here for FP-induced leakage of resealed ghosts (Fig. 3) is similar to that previously reported for FP-induced hemolysis [23]. However, FP-induced leakage is a much more rapid process than FP-mediated hemolysis (Fig. 3 and Mobley et al. [23]); this suggests that FP may lyse intact cells and resealed ghosts through distinct mechanisms. Also, it should be pointed out that the rapid FP-induced leakage of resealed ghosts (Fig. 3) is analogous to the FP-induced burst of leakage noted for SUV [19] or LUV [20] containing acidic liposomes (POPG) at early time points (approx. 10 s), for resealed ghosts and vesicles each suspended in buffers without divalent cations.

The actions of synthetic FP on red cell membranes reported here are broadly supportive of the hypothesis (see Introduction) that the amino terminus of gp41 plays a critical role in HIV fusion and cytolytic processes. Experiments using synthetic peptides assume that relatively short continuous segments (i.e., 'cassettes') exert similar functions, independent of whether these domains exist as isolated peptides or are in the intact virus [30–32]. For example, the HIV-L peptide at the C-terminus of HIV gp41 is an extremely potent cytolytic agent [31], and may be involved in the reduced $CD4^+$ lymphocyte levels seen in AIDS. That such a 'cassette' model may be generally applicable is suggested by studies showing that the fusion activity of the recombinant HIV Nef-27 protein is retained by a synthetic peptide (21 residues) representing the N-terminal domain [33]. The clear advantage of using synthetic peptides in evaluating 'cassette' functions for HIV envelope proteins is that contributions from other viral domains are eliminated. Such a reductionist approach is useful in assessing the role of the N-terminal gp41 domain in HIV-fusion, given the likely participation of other gp41 and gp120 epitopes [14,17,18]. On the other hand, the disadvantage of synthetic peptides is that there is no ab initio guarantee that the conformation of the isolated peptide will be functionally relevant or replicate that of the peptide in the virus. Nevertheless, Jiang et al. [34] reported that rabbit antisera raised to an immunoconjugate of a N-terminal gp41 peptide (residues 518–542) inhibited HIV-1 replication and cell fusion in vitro. This suggests that the synthetic N-terminal gp41 peptide assumes a functionally-relevant conformation.

A critical test of the relevance of the above FP-red cell system in understanding HIV fusion/cytolysis comes from site-directed mutagenesis studies. Since replacement of hydrophobic amino acids with polar residues in the N-terminal domain reduced HIV infectivity and syncytia formation in earlier mutagenic experiments [11–14], it would be important to learn if these substitutions similarly inhibit synthetic peptide-induced red cell fusion and cytolysis. Accordingly, we synthesized a FP analog (FP526L/R) in which Leu at position 526 was replaced with a polar Arg. The FP526L/R analog was chosen because an earlier mutagenic study, using $CD4^+$ HeLa cells transfected with HIV *env* glycoprotein expression vectors, indicated that this substitution blocked syncytium formation; however, this replacement had no effect on gp160 processing, gp120 secretion and CD4 binding [12]. Our finding that

FP526L/R has no fusogenic (Figs. 1 and 6) or lytic (Fig. 3) effects not only indicates that the strongly-conserved N-terminal gp41 domain is involved in HIV-fusion processes, but also confirms that addition of synthetic FP (and FP analogs) to red cells is a useful model for examining these activities.

Our proposal that the fusogenic and/or cytolytic actions of HIV-1 gp41 are retained by the N-terminal peptide (FP) is analogous to that put forward for fusion peptides of related viruses. For example, Schlegel and Wade [35] reported that the synthetic aminoterminal peptide (i.e., 50 μM KFT25; 25 residues) of the G protein of vesicular stomatitis virus (VSV) shows both hemolytic and hemagglutination activities; the fusion and lytic properties of KFT25 parallel those of the G protein from which the peptide is derived. Similarly, Wharton et al. [36] reported that the fusion and lytic properties of the influenza virus haemagglutinin (HA) were mimicked by the amino-terminal peptide (23 residues) derived from the HA_2 subunit. Last, Crane et al. [37] observed that the hydrophobic amino terminal peptide (24 residues) derived from the envelope protein of visna virus caused syncytia formation of goat cells. Antibodies to this peptide inhibited either visna viral-induced cell fusion or peptide-mediated fusion of goat cells. Since the envelope glycoprotein has previously been shown to mediate visna virus fusion, the simplest explanation of these data is that the N-terminal domain retains the fusogenic activity of the whole envelope protein.

Our studies showing that FP fuses red cell membranes suggest mechanisms for not only HIV fusion with $CD4^+$ cells but also the syncytia formation of HIV-infected $CD4^+$ cells. Earlier, a 'dual-receptor' model has been proposed for the participation of HIV infection of cells and syncytia produced by infected cells. The initial binding of HIV to target membranes occurs principally between viral gp120 (glycoprotein 120000) and the CD4 glycoprotein on the host-cell surface [38]. Early experiments indicated that, after this highly specific CD4-gp120 binding (K_D approx. 10^{-9} M), gp120 may break its non-covalent interactions with gp41 and be shed from the viral envelope [39,40]. The dissociation of gp120 may lead to exposure of previously cryptic gp41 sites [39,40] such as an activated N-terminal gp41 peptide, which in turn may attack the host cell surface [10]. More recent work indicates that gp120 shedding may not be integral to the fusion cascade [41,42], and that a gp120 epitope may participate with the N-terminal gp41 domain in HIV fusion [14]. Our prior structural studies [6] indicated that FP binds with relatively low specificity to either lipid or protein sites, or both. The envelope gp41, along with a possible contribution from gp120, could act as a 'bridge,' linking the target cell surface bilayer (through the N-terminal peptide of gp41) with the HIV envelope bilayer (through the embedded gp41 transmembrane sequences) [8]. If the fusogenic activity of synthetic FP reported here were retained by the corresponding peptide in HIV, then it would be anticipated that the N-terminal domain of gp41 could participate in the fusion of the viral envelope with target cell membranes. This 'dual-receptor' model is readily modified to account for how HIV-infected cells, which express gp120 and gp41 on the cell surface, fuse with uninfected CD4-bearing cells to form multicell syncytia.

The results demonstrating FP fusion activity may also account for HIV interactions with, and infection of, cells which do not bear the CD4 receptor. Larsen et al. [43] recently reported that HIV-1 fuses with human erythrocyte ghosts (i.e., non-CD4 bearing cells). Exposed N-terminal gp41 peptides on HIV-1 may bind to human red cell membrane proteins and lipids, thereby inducing fusion of opposing viral and red cell membranes. This fusion process may be somewhat analogous to that observed with synthetic N-terminal gp41 peptides and red cells. A relatively non-specific interaction between FP and target membranes may also explain how HIV infects cells (e.g., fibroblasts and glial cells and apical surfaces of colonic epithelial cells) which do not have CD4 receptors [44–46]. Without the targeting of the highly-specific CD4-gp120 interaction, however, HIV fusion with non-CD4 bearing cells would be expected to be only a minor pathway for viral infection.

Although FP-mediated red cell aggregation (Figs. 6 and 7) appears similar to the multicell syncytia observed in HIV-infected $CD4^+$ cell cultures [47], the precise mechanisms for these fusion processes must be different. For fusion of HIV-infected cells with uninfected cells, the above 'dual-receptor' model argues that host and target cell membranes are fused via the entire gp41 transmembrane protein. However, only the 23-residue amino terminal peptide of HIV-1 gp41 participates in the FP-induced red cell aggregation reported here. Also, it should be noted that FP-induced red cell aggregates (Fig. 7) are more strongly distorted and elongated than the multicell syncytia observed in HIV-infected $CD4^+$-cell cultures [47].

It is important to determine the underlying physical mechanisms by which the N-terminal gp41 peptide induces red cell fusion, aggregation and lysis. Earlier structural studies indicated that nitroxide spin-labeled FP readily inserts into red cell membranes, and is capable of binding to endogenous lipids or proteins, or both [6]. At low FP/red cell lipid ratios (approx. 1:1400), FP assumes a monomeric, α-helical conformation for residues 519–536 and is oriented so that the amino terminus (Ala-519) is buried in the interior of the membrane bilayer and the C-terminal region (Met-537) is in the aqueous environment. At high FP/lipid ratios (approx. 1:200), FP is aggregated into multimeric peptides and adopts both β-strand and α-helical conformations. These FP aggregates may be related to the filamentous structures seen in an electron microscopic study of the HIV-1 N-terminal gp41 peptide in aqueous medium [48]. Since FP aggregates occur at the same doses that trigger hemolysis [6,7,23],

leakage (Fig. 3), fusion (Figs. 1 and 2) and aggregation (Figs. 6 and 7), membrane aggregates of FP may be involved in these processes. For example, FP-induced lytic events may be triggered by the formation of peptide 'pores' that allow ion flux or the creation of non-lamellar lipid [49]. Conceivably, FP aggregates may act to 'tether' adjacent red cells, thereby facilitating both lipid-mixing and multicell formation. It will be of considerable interest in future studies to determine whether the N-terminal gp41 peptide interacts similarly with CD4-bearing cells.

Acknowledgements

We thank the reviewers for their comments, Ms. Carol Leung and Mr. Sigmun Lee for technical assistance, Drs. Kym Faull and Ken Cauglyn (UCLA Center for Molecular and Medical Sciences Mass Spectrometry) for mass spectroscopic analysis of HIV peptides, and Dr. Audrey Fowler (UCLA Protein Microsequencing Facility) for quantitative amino acid analysis of the peptide. This paper fulfills a portion of the requirements of Ms. Hsing-Fang Lee for a M.S. degree (California State Polytechnic University, Pomona, CA, USA). We gratefully acknowledge support by Charles R. Drew University of Medicine and Science (AJW), NIH Grants GM 08140 and RCMI G12 RR 3026 (LMG, AJW) the AMHPS AIDS Research Consortium-NIH Grant 5P20 A129360-03 (LMG, AJW), NIH Small Equipment Grant GM 50483 (AJW, LMG) and Commonwealth AIDS Research Grant AG201 (CCC).

References

[1] Myers, G., Korber, B., Berzofsky, J.A., Smith, R.F. and Pavalakis, G.N. (1991) in Human Retroviruses and AIDS 1991: A Compilation and Analysis of Nucleic Acid and Amino Acid Sequences, pp. II–81, Los Alamos National Lab., Los Alamos, NM.
[2] McCune, J.M., Rabin, L.B., Feinberg, M.B., Lieberman, M., Kosek, J.C., Reyes, G.R. and Weisman, I.L. (1988) Cell 53, 55–67.
[3] White, J., Killian, M. and Helenius, A. (1983) Q. Rev. Biophys. 16, 151–195.
[4] Gallaher, W.R. (1987) Cell 50, 327–328.
[5] Gonzalez-Scarano, F., Waxham, M.N., Ross, A.M. and Hoxie, J.A. (1987) AIDS Res. Hum. Retroviruses 3, 245–252.
[6] Gordon, L.M., Curtain, C.C., Zhong, Y.C., Kirkpatrick, A., Mobley, P.W. and Waring, A.J. (1992) Biochim. Biophys. Acta 1139, 257–274.
[7] Gordon, L.M., Curtain, C.C., McCloyn, V., Kirkpatrick, A., Mobley, P.W. and Waring, A.J. (1993) AIDS Res. Human Retroviruses 9, 1145–1156.
[8] Aloia, R.C., Jensen, F.C., Curtain, C.C., Mobley, P.W. and Gordon, L.M. (1988) Proc. Natl. Acad. Sci. USA 85, 900–904.
[9] Gordon, L.M., Jensen, F.C., Curtain, C.C., Mobley, P.W. and Aloia, R.C. (1988) Biochim. Biophys. Acta 943, 331–342.
[10] Koenig, S., Hirsch, V.M., Olmsted, R.A., Powell, D., Maury, W., Rabson, A., Fauci, A.S., Purcell, R.H. and Johnson, P.R. (1989) Proc. Natl. Acad. Sci. USA 86, 2443–2447.
[11] Felser, J., Klimkait, T. and Silver, J. (1989) Virology 170, 566–570.
[12] Freed, E.O., Myers, D.J. and Risser, R. (1990) Proc. Natl. Acad. Sci. USA 87, 4650–4654.
[13] Freed, E.O., Delwart, E.L., Buchschacher Jr., G.L. and Panganiban, A.T. (1992) Proc. Natl. Acad. Sci. USA 89, 70–74.
[14] Bergeron, L., Sullivan, N. and Sodroski, J. (1992) J. Virol. 66, 2389–2397.
[15] Kowalski, M., Bergerom, L., Dorfman, T., Haseltine, W. and Sodroski, J. (1991) J. Virol. 65, 281–291.
[16] Larsen, C., Ellens, H. and Bentz, J. (1992) in Advances in Membrane Fluidity (Aloia, R.C. and Curtain C.C., eds.), Vol. 6, pp. 143–166, Wiley-Liss, New York.
[17] Helseth, E., Olshevsky, U., Gabuzda, D., Ardman, B., Haseltine, W. and Sodroski, J. (1990) J. Virol. 64, 6314–6318.
[18] Owens, R.J., Burke, C. and Rose, J.K. (1994) J. Virol. 68, 570–574.
[19] Rafalski, M., Lear, J.D. and DeGrado, W.F. (1990) Biochemistry 29, 7917–7922.
[20] Nieva, J.L., Nir, S., Muga, A., Goñi, F.M. and Wilschut, J. (1994) Biochemistry 33, 3201–3209.
[21] Martin, I., Defrise-Quertan F., Decroly, E., Vandenbranden, M., Brasseur, R. and Ruysschaert, J.-M. (1993) Biochim. Biophys. Acta 1145, 124–133.
[22] Slepushkin, V.A., Melikyan, G.B., Sidorova, M.S., Chumakov, V.M., Andreev, S.M., Manukyan, R.A. and Karamov, E.V. (1990) Biochem. Biophys. Res. Commun. 172, 952–957.
[23] Mobley, P.W., Curtain, C.C., Kirkpatrick, A., Rostamkhani, M., Waring, A.J. and Gordon, L.M. (1992) Biochim. Biophys. Acta 1139, 251–256.
[24] Gordon, L.M. and Mobley, P.W. (1984) J. Membr. Biol. 79, 75–86.
[25] Sze, H. and Solomon, A.K. (1979) Biochim. Biophys. Acta 550, 393–406.
[26] Hoekstra, D., de Boer, T., Klappe, K. and Wilschut, J. (1984) Biochemistry 23, 5675–5681.
[27] Ellens, H., Bentz, J. and Szoka, F.C. (1985) Biochemistry 24, 2099–3106.
[28] Birch, D.F., Fairley, K.F., Whitworth, J.A., Forbes, I., Fairley, J.K., Chesire, G.R. and Ryan, G.B. (1983) Clin. Nephrology 20, 78–84.
[29] Hoekstra, D., Wilschut, J. and Scherphof, G. (1983) Biochim. Biophys. Acta 732, 327–331.
[30] Gallaher, W.R., Ball, J.M., Garry, R.F., Griffin, M.C. and Montelaro, R.C. (1989) AIDS Res Hum. Retroviruses 5, 431–440.
[31] Miller, M.A., Garry, R.F., Jaynes, J.M. and Montelaro, R.C. (1991) AIDS Res. Hum. Retroviruses 7, 511–519.
[32] Miller, M.A. and Montelaro, R.C. (1992) in Advances in Membrane Fluidity (Aloia, R.C. and Curtain, C.C., eds.), Vol. 6, pp. 351–364, Wiley-Liss, New York.
[33] Curtain, C.C., Separovic, F., Rivett, D., Kirkpatrick, A., Waring, A.J., Gordon, L.M. and Azad, A.A. (1994) AIDS Res. Hum. Retroviruses 10, 1231–1240.
[34] Jiang, S., Lin, K., Strick, N. and Neurath, A.R. (1993) Biochem. Biophys. Res. Commun. 195, 533–538.
[35] Schlegel, R. and Wade, M. (1985) J. Virol. 53, 319–323.
[36] Wharton, S.A., Martin, S.R., Ruigrok, R.W.H., Skehel, J.J. and Wiley, D.C. (1988) J. Gen. Virol. 69, 1847–1857.
[37] Crane, S.E., Kanda, P. and Clements, J.E. (1991) Virology 185, 488–492.
[38] Lasky, L.A., Nakamura, G., Smith, D.H., Fennie, C., Shimasaki, C., Patzer, E., Berman, P., Gregory, T. and Capon, D.J. (1987) Cell 50, 975–985.
[39] Moore, J.P., McKeating, J.A., Norton, W.A. and Sattentau, Q.J. (1991) J. Virol. 250, 1139–1142.
[40] Hart, T.K., Kirsh, R., Ellens, H., Sweet, R.W., Lambert, D.M., Petteway, S.R., Leary, J. and Bugelski, P.J. (1991) Proc. Natl. Acad. Sci. USA 88, 2189–2193.
[41] Fu, Y.-K., Hart, T.K., Jonak, Z.L. and Bugelski, P.J. (1993) J. Virol. 67, 3818–3825.
[42] Marcon, L. and Sodroski, J. (1994) J. Virol. 68, 1977–1982.

[43] Larsen, C.E., Nir, S., Alford, D.R., Jennings, M., Lee, K.-D. and Düzgüneş, N. (1993) Biochim. Biophys. Acta 1147, 223–236.
[44] Cheng-Mayer, C., Rutka, J.T., Rosenblum, M.L., McHugh, T., Stites, D.P. and Levy, J.A. (1987) Proc. Natl. Acad. Sci. USA 84, 3526–3530.
[45] Fantini, J., Yahi, N. and Chermann, J.C. (1991) Proc. Natl. Acad. Sci. USA 88, 9297–9301.
[46] Tateno, M., Gonzalez-Scarano, F. and Levy, J.A. (1989) Proc. Natl. Acad. Sci. USA 86, 4287–4290.
[47] Resnick, L. and Novatt, G. (1986) J. Amer. Med. Assoc. 255, 3421.
[48] Slepushkin, V.A., Kornilaeva, G.V., Andreev, S.M., Sidorova, M.S., Petrukhina, A.O., Matsevich, G.R., Raduk, S.V., Grigoriev, V.B., Makarova, T.V., Lukashov, V.V. and Karamov, E.V. (1993) Virology 194, 294–301.
[49] Epand, R.M., Cheetham, J.J., Epand, R.F., Yeagle, P.L., Richardson, C.D., Rockwell, A. and DeGrado W.F. (1992) Biopolymers 32, 309–314.